The Regime Shift Detector: a model to identify changes in dynamic rules governing populations

C.A. Bahlai[1,2] And E.F. Zipkin[2]

1 Department of Biological Sciences, Kent State University. Kent, Ohio, United States of America. Email for correspondence: cbahlai@kent.edu

2 Department of Integrative Biology; Program in Ecology, Evolutionary Biology and Behavior, Michigan State University, East Lansing, Michigan, United States of America.

Abstract

1: Environmental factors may interact with internal rules of population regulation, sometimes perturbing systems to alternate dynamic states. Yet, pinpointing when state changes occur in naturally fluctuating populations is difficult. An analytical approach that can identify the timing and magnitude of such changes, or "regime shifts", would facilitate understanding of abrupt ecological transitions with potential to inform conservation and management of species.

2: We developed a generalizable model, the "Regime Shift Detector", for identifying changes in the parameters of a simple density dependent model governing the temporal fluctuations of a population. The model is a tool comprised of a suite of functions for examining population time series data for the presence, location, and magnitude of parameter shifts. The model uses an iterative approach to fitting subsets of time series data, then ranks the fit of a particular break point combination using model selection and assigns a relative weight to each break. We examined the performance of this model with simulations and two case studies: the invasion of the multicolored Asian ladybeetle and the decline of the eastern monarch butterfly.

3: We found that under low environmental/sampling noise, the break point sets selected by the Regime Shift Detector contained the true simulated breaks with 70-100% accuracy, with the most complex parameterization conditions (i.e. time series with many break points) least likely to be detected by the model. The weighting tool generally assigned breaks intentionally placed in simulated data (i.e., true breaks) with weights averaging >0.8 and those due to sampling error (i.e., erroneous breaks) <0.2, although the absolute weights of true versus erroneous breaks found by the model varied somewhat with other simulation parameters.

4: In our case study examining the invasion process of ladybeetles, the Regime Shift Detector identified shifts in population cycling associated with variation in prey availability. The shifts identified for the eastern monarch population were more ambiguous, but generally coincided with changing management practices affecting the availability of hostplants in their summer breeding grounds.

5: The Regime Shift Detector identifies possible break points within time series data and quantifies the strength of evidence for each break point. When interpreted in the context of species biology, the Regime Shift Detector has the potential to aid management decisions and identify critical time periods related to species' dynamics. In an era of rapid global change, such tools can improve understanding of the conditions under which population dynamics shift to other states.

Introduction

Population dynamics are governed by internal, biotic rules and also external abiotic factors, leading to both stochastic and deterministic forces governing abundance patterns (Bjørnstad and Grenfell 2001). External perturbations to population processes can lead to regime shifts, where the internal rules that govern fluctuations in population abundance transition to another state (Hare and Mantua 2000, Carpenter et al. 2008). Understanding how and when external environmental factors interact with internal density dependent regulation remains a fundamental challenge in population ecology (Sutherland et al. 2013, Eason et al. 2016).

Density dependent tools for modelling population time series were developed and championed during the 1950s and 60s. Examples include the Ricker and Beverton-Holt models, which were initially developed for fisheries management and describe the expected population size in year *t* as a function of the population size in year *t*-1 (Ricker 1954, Beverton and Holt 1957). The accuracy of these simple density dependent models is generally highest for populations fluctuating around their carrying capacity (Sabo et al. 2004), with compensatory density dependence and no lag effects (Bjørnstad and Grenfell 2001). Although this deterministic approach to population modelling has largely fallen out of favor for more complex structures and stochastic elements (May 1976, Barraquand et al. 2017, Boettiger 2018), simple dynamic models remain useful, largely due to their easily interpretably and ecologically meaningful parameters (Gadrich and Katriel 2016). Differences in parameter values between populations, or a change within a single population, can suggest differences in environmental constraints governing a population, providing a quantifiable effect of environmental change (Forchhammer and Asferg 2000, Berryman and Lima 2006, Zipkin et al. 2009, Bahlai, vander Werf, et al. 2015).

Although theoretically straightforward, identifying abrupt transitions in ecological systems is challenging using real-world data due to a lack of systematic approaches and noise in naturally produced time series data (Bestelmeyer et al. 2011). In many cases, transition points are applied to time series data *ad hoc*, based on data visualization or specific hypotheses surrounding factors affecting population fluctuations (Hare and Mantua 2000, Toms and Lesperance 2003, Weimerskirch et al. 2003, Berryman and Lima 2006, Knapp et al. 2012), creating the potential for biases in selecting break points. Break point analysis tools eliminate this bias by locating change points with a variety of optimization strategies, including linear and moving average methods (Braun and Muller 1998, Zeileis et al. 2001, Killick and Eckley 2014, Priyadarshana and Sofronov 2015). However, these methods do not work on data with internal, density dependent structure inherent to population time series. Density-dependent population growth has the potential to mask transition points. For example, transient dynamics occurring immediately after a temporary disturbance can result in a change in population size, but not necessarily in the rules governing population fluctuations. Wavelet analysis has been applied to population time series to address changes in cycling patterns (Jenouvrier et al. 2005) but this method also does not account for density-dependent processes as an explicit mechanism governing changes in abundance (Cazelles et al. 2008). A robust, unbiased tool for detecting regime shifts would simultaneously allow us to identify when shifts in population cycling processes occur and further quantify the specific changes to the underlying dynamics driving populations.

In this paper, we develop a generalizable tool, the Regime Shift Detector (RSD), for identifying shifts in dynamic regimes within density-dependent populations using time series data. We illustrate our

approach using the Ricker model because of its simplicity and high performance under a variety of realistic environmental scenarios. Yet, the techniques described in our paper can be readily adapted for other model structures, including more complicated processes such as seasonal periodicity or lag effects. We describe the basic structure of our model and how it can be used to evaluate the presence, location, and magnitude of shifts in population parameters governing dynamics. We demonstrate the utility of our model through a series of simulations and apply the model to real-world case studies of two populations of conservation and economic concern. First, we examine the invasion process of the multicolored Asian ladybeetle (*Harmonia axyridis*), a cosmopolitan invasive, in the two decades following its arrival in Midwestern US agricultural ecosystems. Then, we examine the declining eastern monarch butterfly (*Danaus plexippus*) population using census data collected on its overwintering grounds in Mexico over a similar two decade period. In our ladybeetle case study, the RSD model identified shifts in population cycling associated with known variation in prey availability, with moderately high weight associated with a break coinciding with prey arrival and a moderately low weight associated with a break coinciding with management actions against the prey. The results for the monarch population were more ambiguous, with greater uncertainty about the number and location of breaks in the time series. Several equivalently performing break point combinations had divergent weights associated with their specific break points, suggesting multiple, super-imposed biological processes driving the dynamics of this species.

The Regime Shift Detector model

For the purposes of our analyses, we assume that the population of interest follows a Ricker model structure such that the population size in time t+1, N_{t+1}, is dependent on the population size in time t, N_t, the carrying capacity of the system, K, and the per-capita annual growth rate, r (Turchin 2003):

$$N_{t+1} = N_t \exp\left(r\left(1 - \frac{N_t}{K}\right)\right) + \varepsilon_t.$$

We further assume that observed annual population abundance is partially stochastic and may be influenced by either environmental variation and/or sampling error. We include an error term ε_t to represent this noise, which follows a normal distribution centered around zero with a variance of σ^2. The parameters K, r, and ε_t are estimated from the population time series data (N_1, N_2, … N_t). The Ricker model is a useful starting point for breakpoint analyses because 1) it does not rely on any external information (abundance in time *t* is a function of only abundance in time *t*-1); 2) only three parameters need to be estimated, and those parameters have ecologically meaningful interpretations; and 3) it is an extremely flexible distribution, taking a variety of forms, from linear to compensatory to over-compensatory, and thus has a wide range of applications across a variety of taxa (Ricker 1954, Brook and Bradshaw 2006).

To build the RSD model, we use an iterative, model-selection process to determine if, and when, shifts in parameter values occur within a given time series. To achieve this, we first fit the Ricker model to the entire time series of available data. Then the population time series is subdivided into all possible combinations of 2, 3, …, n subsets of sequential data points (hereafter, 'break point combinations') and the Ricker model is fit to each of the subsets produced for each break point combination. To avoid overfitting, we constrain break point combinations to include only subsets with a minimum of four sequential data points.

After fitting all break point combinations, we evaluate the candidate set of models by calculating the Akaike Information Criteria for small sample sizes (AICc) value for each segment and summing them accordingly (Hall et al. 2013). Fits for break point combinations with comparatively lower AICc values are considered to have better performance. For a given time series, the RSD model produces a set of top performing break point combinations for cases in which model fits produce equivalent AICc values (i.e. within 2 units of the best-performing fit; Burnham and Anderson 2002). To evaluate the strength of evidence for an identified break in the time series, we use the relative variable importance method (Burnham and Anderson 2002). To do this, we compute the Akaike weight w_i for every identified break point across all combinations and sum the Akaike weights for the break point across all possible break point combinations with Akaike weights >0.001. Break point combinations with weights <0.001 were excluded to increase computational efficiency. We selected AICc as our information criterion for model selection within the RSD model because it provides a balance of specificity and sensitivity. However, we also completed a parallel analysis with an identical procedure using AIC as the information criterion for decision-making, which is documented in Appendix S1 (and not discussed again in the main text). AICc is a function of AIC with a correction for small sample bias, which is appropriate for the sample sizes typical to contemporary population time series data (i.e., 15-30 years/data points) and is designed to minimize the risk of overfitting during model selection (Burnham and Anderson 2002). However, use of AIC for model selection may be desirable when increased model sensitivity to dynamic shifts is desired.

The RSD model is implemented as a series of R functions to enable a user to quickly generate a list of potential break points for a population time series dataset. The model (and all subsequent simulations and case studies) were scripted and run in R Version 3.3.3 (R Development Core Team 2017). All data manipulations, analyses and figure scripts, including the complete development history, are publicly available in a Github repository at https://github.com/cbahlai/monarch_regime. We summarize the role of each function used in the model within Appendix S2.

Simulation study

We conducted a series of simulations to test the accuracy of the RSD model under a variety of plausible parameter spaces. For all scenarios, we fix N_1 = 3000, and K = 2000 in the initial conditions, as the Ricker model is most reliably fit for populations fluctuating around their carrying capacity. As the dynamic observed in a Ricker population is driven primarily by the relationship of other parameters to K than by the absolute value of K itself, we held the starting value of K constant for all simulations. For each set of simulations, we held the variables not being varied at "base values" defined as: starting value of r = 2, change in r = ±25%, change in K = ±75%, 2% noise (τ; described below), with time series length of 20 years. We examined the effect of the size of initial r on model performance by creating scenarios with different starting values of r = 0.5, 1, 1.5, 2. For each value of initial r, we modified the percent change in r at break points from the starting values (± no change, 10%, 25%, 50%, 75%) while holding all other parameters at base values. We then ran a set of simulations examining the percent change in K at break points from its starting value (± no change, 10%, 25%, 50%, 75%) while holding all other parameters (including r) at base values. This lead to a total of 40 scenarios (four starting values of r with five percent changes in r and five percent changes in K). We further evaluated how the magnitude of stochasticity in the system (as measured by the error term ε_t) influenced model performance. For generalizability of our simulation results, we simulated error as a percentage of the mean population size, rather than as absolute value (as described in the model above that we used for fitting the RSD). For each annual population size in the simulated dataset, a random value was selected from a normal curve of mean 0

and standard deviation of τ (where τ = 1%, 2%, 5%, 10%, 15%) and multiplied by the expected population size generated from the deterministic portion of the model. We ran these simulations with all noise (τ) levels across all percent change values for *r* and *K* (with other parameters held at base values) for a total of additional 50 scenarios (five percent noise values with five percent changes in *r* and five percent changes in *K*). Finally, we also tested the impact of time series length by modifying the length of the simulated time series at five-year intervals over a range from 15 – 30 years (as the number of break point allows) while holding all other parameters constant, for four additional scenarios. We generated 250 simulated datasets for each of the 94 possible scenarios assuming breakpoint combinations with 0, 1, 2 and 3 breaks. Break point locations were randomly selected from within the set of possible time points. In total, we generated 93,572 data sets that we examined with our RSD model. (Note that 94,000 simulations were run but simulations for higher numbers of break points in shorter time series occasionally failed; results for such combinations are not presented).

We evaluated the RSD model's performance for all test scenarios by examining its ability to identify the true break points within the set of the best fitting break point combinations (i.e. the top ranked break point combination and those break point combinations whose AICc values fell within two units of the top ranked). We also examined the performance of the break-point weighting tool by calculating the average weightings of all true and erroneous break points identified in the top performing model(s) across all runs of a given scenario.

The scenario with the correct number of breaks and their locations was detected within the top performing break point combination sets with >70% accuracy under nearly all parameterizations (Fig. 1). The accuracy was generally lowest in time series with three break points but above 70% for most scenarios. These results remained roughly consistent regardless of the value of the variance (σ^2) determining the annual amount of environmental/sampling noise (Fig. 1 A). Results were similar across all r values tested but performance of the RSD declined slightly when initial *r* was large (>2.0; Fig. 1 B). The RSD model had the highest accuracy with larger shifts in K (≥25%; Fig 1. C) and relatively smaller changes to *r* (≤25%; Fig. 1 D). This result is somewhat counter-intuitive, as we would generally expect large shifts in all parameters to be more easily detected. However, because the Ricker model produces chaotic dynamics with high values of r (r > 2.3) a large shift in parameters could potentially result in a situation where multiple break point fits would perform equally well. Finally, the accuracy of the RSD model decreased as scenario length increased, likely because of the factorial increase in potential break point combinations with additional data in the time series (Fig. 1 E). Accuracy was also low in cases where the number of break points was high relative to the time series length (e.g., 20 years and three breaks).

The breakpoint weighting analysis revealed that in the vast majority of cases, the average weight of a true break exceeded a value of 0.8 (Fig. 2A-E), whereas the weight of erroneous breaks averaged less than 0.2 in weight. The notable exception occurred when true breaks resulted from very small shifts in K (Fig. 2 C). Thus, when a weight of >0.8 is indicated for a break found by the RSD model, we can reasonably conclude this is a true break, and likewise, a break with a weight of <0.2 can reasonably assumed to be erroneous. Weight values intermediate to those two thresholds can be interpreted as a quantification of the strength of evidence that a break occurred.

Applications

We tested the performance of the RSD model with two cases using population time series data from field observation studies. Both case studies involve approximately two decades of observations of economically or culturally important insect species: one case examines an invasion process and the other examines a population decline, both occurring over the same time period in recent history.

Multicolored Asian ladybeetles in southwestern Michigan

The 1994 invasion of multicolored Asian ladybeetles to southwestern Michigan, United States was documented in monitoring data collected on agriculturally-important Coccinellidae (ladybeetles) in landscapes dominated by field crops. Population density of ladybeetles is monitored in ten plant communities weekly over the growing season using yellow sticky card glue traps starting in 1989 at the Kellogg Biological Station at Michigan State University. We used data on the captures of adults at the site from 1994-2017, culled at day of year 222 (August 10) to minimize the effect of year-to-year variation in the sampling period. We then calculated the average number of adults captured per trap, across all traps deployed within a sampling year, and used this value in our analysis. Detailed sampling methodology is available in previous work (Bahlai et al. 2013, Bahlai, Colunga-Garcia, et al. 2015, Bahlai, vander Werf, et al. 2015).

Two break points, one occurring after 2000 and one occurring after 2005, were observed in the top break point combination model (Fig. 3 A, AICc=-18.02). However, the RSD model indicated that two additional break point combinations, a single break after 2000 (AICc=-17.46), and a no break series (AICc=-17.64), had equivalent performance. Break weight analysis suggested a weight of 0.56 for the 2000 break, and a weight of 0.29 for the break after 2005. As these weights fall into a range intermediate to our 0.2 and 0.8 decision rules, we conclude that there is reasonably strong evidence of a shift in dynamic rule after 2000, and moderate-weak evidence for a shift after 2005. The shift in 2000 is characterized by substantial increases in the values of *K* and *r*, with approximate increases of 75% and 40% over their initial estimates, respectively (Table 1). The shift in 2005 is characterized by a return to parameter estimates that were nearly identical to those observed at the beginning of the time series (Table 1, Fig. 3 B).

These observations can be explained in the context of the known ecology of this ladybeetle. Dynamics of the ladybeetle invasion appear to be closely coupled with prey availability (Bahlai and Sears 2009, Heimpel et al. 2010, Rhainds et al. 2010, Bahlai, Colunga-Garcia, et al. 2015), which, in turn, is driven by documented pest management practices (neonicotinoid insecticide use; Bahlai, vander Werf, et al. 2015) leading to a relatively simple pulsed change. The first shift in the dynamics of the Asian ladybeetle, after 2000, corresponds to the well documented arrival and establishment of soybean aphid to North America, a preferred prey item from the ladybeetle's native range (Ragsdale et al. 2004, Wu et al. 2004). The invasion of this aphid dramatically increased resources available to the ladybeetle in habitats where the beetles were already well-established (Bahlai et al. 2013), supporting both a higher carrying capacity and a greater intrinsic growth rate. The second shift, after 2005, was less strongly supported, but coincides with the introduction and uptake of a management strategy for aphids that incompletely controlled the prey item. Landscape-scale use of neonicotinoid insecticides decreased prey numbers, particularly during the spring when aphids colonize new hosts, which could be limiting early season reproduction of ladybeetles (Bahlai, vander Werf, et al. 2015). Indeed, in this case, we would expect a weaker shift in dynamics as the prey item is incompletely controlled, and control tactics were not uniformly adopted across the prey's range all at one time.

Monarch butterflies in Mexican overwintering grounds

The eastern population of the North American monarch butterfly (*Danaus plexippus*) is migratory, with the majority of individuals overwintering in large aggregations in Oyamel fir forests within the transvolcanic mountains in the central region of Mexico (Urquhart and Urquhart 1978). Monarchs are highly dispersed over their breeding season, occupying landscapes throughout the agricultural belt in central and eastern United States and southern Canada (Flockhart et al. 2017). As such, estimates of the overwintering population size can provide a convenient and inclusive annual metric of the size of the eastern migratory population (Prysby and Oberhauser 2004). This population of monarchs has been in dramatic decline in recent decades, although the degree and cause of this decline is hotly debated (Sarkar 2017). We used data on the total area occupied by monarchs from 1995-2017 (based on early winter surveys conducted in December) compiled by the World Wildlife Fund Mexico (available at MonarchWatch; Lovett 2017).

The RSD model estimated that the best break point combination fit for the monarch overwintering data was a single break after 2003 (Fig. 4; AICc=120.18). However, the model indicated that two additional break point combinations, a single break after 2006 (AICc=121.87) and a two-break combination of 2003 and 2008 (AICc=-121.86), had equivalent performance. The weight analysis computed weights of 0.49, 0.14, and 0.26, for 2003, 2006, and 2008 respectively, suggesting that the break at 2006 is unlikely. But there is intermediate support for the 2003 and 2008 breaks. As with our ladybeetle case study, the strength of evidence was strongest for the first break in 2003, and weaker for the second break. The shift corresponds with a >50% reduction in K in 2003, and, if the secondary break is taken at 2008, a further reduction of K nearing 50% again at that point (Table 1; Fig. 4 B).

The patterns we observe are consistent with a leading hypothesis to explain monarch population decline. Loss of milkweed hostplants due to changing agricultural practices on Midwestern breeding grounds (Hartzler 2010, Pleasants and Oberhauser 2013) is hypothesized to be a major driver in the dynamics of this species. Changing herbicide practices in central North America have largely eliminated milkweed hostplants from agricultural field crops, with fairly consistent, low levels of milkweed on the landscape starting from about 2003-2005 (Zaya et al. 2017). Although glyphosate tolerant soybeans and maize were introduced to the US market in 1996 and 1998 respectively (Duke and Powles 2009), actual glyphosate use lagged behind, with dramatic increases in use of the pesticide in 1998- 2003 in soybean, and 2007-2008 in maize (Baker 2017).

However, additional drivers likely also play a role in monarch processes given the uncertainty in our results. Abiotic drivers of monarch population dynamics are complex and can interact at local, regional, and continental scales (Saunders et al. 2017). Other studies have implicated climate (Zipkin et al. 2012), extreme weather events (Brower et al. 2004), changing habitat availability on wintering grounds (Vidal and Rendón-Salinas 2014), and mortality during the fall migration (Davis and Altizer 2015) as possible factors influencing monarch population dynamics. With many super-imposed drivers, monarch dynamics are likely driven by both press and pulsed processes, making the detection of discrete break points associated with regime shifts complicated.

Discussion

The RSD model provides a novel and objective tool for evaluating changes in parameter values that govern natural populations, such as carrying capacity and population growth rates. As illustrated with

our simulations and case studies, the RSD model can not only identify and quantify parameters changes but also provide insight into system drivers and help detect time frames where research should be focused more closely. We recommend that the model selection approach be used to identify a list of potential break points and break point combinations and the weighting tool be used to evaluate the strength of evidence for each potential break, providing a clear direction to focus downstream research on changing dynamic processes.

The performance of the RSD model was relatively stable among the break point simulations we tested. We found that the amount of environmental/sampling noise (ranging from 1-15%) had little effect on model performance (Fig. 1 A). Other input conditions had relatively greater impacts on the performance of the RSD model, depending on which parameter was changed and by how much. Large shifts in *K* were more easily detected than smaller shifts (Fig. 1 C). However, large changes in *r* were harder to detect, but this effect varied by parameterization complexity (Figs. 1, 2 D). Although larger shifts in regression parameters would, intuitively, lead to a higher likelihood of detection, large shifts in *r* are also more likely to induce large variations in transient dynamics in the years immediately following the shift, potentially making the timing of shifts more difficult to pinpoint. Similarly, longer time series yielded results that were more error prone (Fig. 1-2 E). This is likely because there were simply more possible break-point combinations for the model to select from and because the penalty for increasing parameterization (i.e. AICc) decreases as sample sizes grow (leading to increasing likelihood of identifying extra, erroneous breaks).

In applying these insights to our case studies, we found interpretation of the ladybeetle example was relatively straightforward (Fig. 3). Our top break point combination and the equivalently-performing set did not contain contradictory information: each candidate set was simply a subset of breakpoints from the most complex set, and only two break points were found. Both of these break points were associated with moderate or greater weights, although the values of these break weights were in the intermediate range (i.e., between 0.2 and 0.8), suggesting breaks in natural systems may not be as well behaved as those in simulated data. The monarch butterfly case study results were slightly more ambiguous, as the model selection tool identified a break that the weighting tool indicated to be erroneous (Fig. 4). Weights of the two most strongly-supported breaks were numerically similar to those of the ladybeetle case study, and are also interpretable with knowledge of the study system. However, the model selection results suggest additional, superimposed processes may be affecting monarch population dynamics and creating a noisier signal.

We recommend users carefully consider the limitations of the RSD model in the context of their own data. For example, if changes to parameter values occur frequently (e.g., less than 3-4 years or time periods), the frequency of shifts would violate the constraints placed on our model to prevent overfitting. We also observed that the likelihood of identifying erroneous break points increased as time series length increased. Thus, in cases where a long time series exists, but a particular time period is of interest, the RSD model could be used on the time period of interest alone to minimize the likelihood of distracting or erroneous results.

The RSD model functions as a method for identifying break points within time series data and quantifying the strength of evidence for each potential break point. We illustrated our approach with the Ricker model as the functional form governing population dynamics. However, the central dynamic model could be changed or modified to incorporate other, more complicated population processes.

When interpreted in the context of species biology, the RSD model has the potential to aid management decisions, identify critical drivers of change in species' dynamics, and help determine where best to focus additional research efforts.

References

Bahlai, C. A., M. Colunga-Garcia, S. H. Gage, and D. A. Landis. **2013**. Long term functional dynamics of an aphidophagous coccinellid community are unchanged in response to repeated invasion. PLoS One. 8: e83407.

Bahlai, C. A., and M. K. Sears. **2009**. Population dynamics of Harmonia axyridis and Aphis glycines in Niagara Peninsula soybean fields and vineyards. Journal of the Entomological Society of Ontario. 140: 27–39.

Bahlai, C. A., W. vander Werf, M. O'Neal, L. Hemerik, and D. A. Landis. **2015**. Shifts in dynamic regime of an invasive lady beetle are linked to the invasion and insecticidal management of its prey. Ecological Applications.

Bahlai, C., M. Colunga-Garcia, S. Gage, and D. Landis. **2015**. The role of exotic ladybeetles in the decline of native ladybeetle populations: evidence from long-term monitoring. Biol Invasions. 17: 1005–1024.

Baker, N. T. 2017. Estimated annual agricultural pesticide use by crop group for states of the conterminous United States, 1992-2014. National Water Quality Assessment Program.

Barraquand, F., S. Louca, K. C. Abbott, C. A. Cobbold, F. Cordoleani, D. L. DeAngelis, B. D. Elderd, J. W. Fox, P. Greenwood, and F. M. Hilker. **2017**. Moving forward in circles: challenges and opportunities in modelling population cycles. Ecology letters. 20: 1074–1092.

Berryman, A., and M. Lima. **2006**. Deciphering the effects of climate on animal populations: diagnostic analysis provides new interpretation of Soay sheep dynamics. The American Naturalist. 168: 784–795.

Bestelmeyer, B. T., A. M. Ellison, W. R. Fraser, K. B. Gorman, S. J. Holbrook, C. M. Laney, M. D. Ohman, D. P. C. Peters, F. C. Pillsbury, A. Rassweiler, R. J. Schmitt, and S. Sharma. **2011**. Analysis of abrupt transitions in ecological systems. Ecosphere. 2: art129.

Beverton, R. J., and S. J. Holt. **1957**. On the dynamics of exploited fish populations. Springer Science & Business Media.

Bjørnstad, O. N., and B. T. Grenfell. **2001**. Noisy Clockwork: Time Series Analysis of Population Fluctuations in Animals. Science. 293: 638.

Boettiger, C. 2018. From noise to knowledge: how randomness generates novel phenomena and reveals information. Ecology Letters. 21: 1255–1267.

Braun, J. V., and H.-G. Muller. **1998**. Statistical Methods for DNA Sequence Segmentation. Statistical Science. 13: 142–162.

Brook, B. W., and C. J. Bradshaw. **2006**. Strength of evidence for density dependence in abundance time series of 1198 species. Ecology. 87: 1445–1451.

Brower, L. P., D. R. Kust, E. Rendon-Salinas, E. G. Serrano, K. R. Kust, J. Miller, C. Fernandez del Rey, and K. Pape. **2004**. Catastrophic winter storm mortality of monarch butterflies in Mexico during January 2002. The Monarch butterfly: biology and conservation. 151–166.

Burnham, K. P., and D. R. Anderson. **2002**. Model selection and multimodal inference: a practical information-theoretic approach, 2nd ed. Springer Science + Business Media, LLC, New York.

Carpenter, S. R., W. A. Brock, J. J. Cole, J. F. Kitchell, and M. L. Pace. **2008**. Leading indicators of trophic cascades. Ecology Letters. 11: 128–138.

Cazelles, B., M. Chavez, D. Berteaux, F. Ménard, J. O. Vik, S. Jenouvrier, and N. C. Stenseth. **2008**. Wavelet analysis of ecological time series. Oecologia. 156: 287–304.

Davis, A. K., and S. Altizer. **2015**. New Perspectives on Monarch Migration, Evolution, and Population Biology. Monarchs in a Changing World: Biology and Conservation of an Iconic Butterfly. 203.

Duke, S. O., and S. B. Powles. **2009**. Glyphosate-resistant crops and weeds: now and in the future. AgBioForum. 12: 346–357.

Eason, T., A. S. Garmestani, C. A. Stow, C. Rojo, M. Alvarez-Cobelas, and H. Cabezas. **2016**. Managing for resilience: an information theory-based approach to assessing ecosystems. J Appl Ecol. 53: 656–665.

Flockhart, D. T. T., L. P. Brower, M. I. Ramirez, K. A. Hobson, L. I. Wassenaar, S. Altizer, and D. R. Norris. **2017**. Regional climate on the breeding grounds predicts variation in the natal origin of monarch butterflies overwintering in Mexico over 38 years. Glob Change Biol. 23: 2565–2576.

Forchhammer, M. C., and T. Asferg. **2000**. Invading parasites cause a structural shift in red fox dynamics. Proceedings of the Royal Society of London B: Biological Sciences. 267: 779–786.

Gadrich, T., and G. Katriel. **2016**. A Mechanistic Stochastic Ricker Model: Analytical and Numerical Investigations. Int. J. Bifurcation Chaos. 26: 1650067.

Hall, A. R., D. R. Osborn, and N. Sakkas. **2013**. Inference on Structural Breaks using Information Criteria. The Manchester School. 81: 54–81.

Hare, S. R., and N. J. Mantua. **2000**. Empirical evidence for North Pacific regime shifts in 1977 and 1989. Progress in Oceanography. 47: 103–145.

Hartzler, R. G. 2010. Reduction in common milkweed (Asclepias syriaca) occurrence in Iowa cropland from 1999 to 2009. Crop Protection. 29: 1542–1544.

Heimpel, G., L. Frelich, D. Landis, K. Hopper, K. Hoelmer, Z. Sezen, M. Asplen, and K. Wu. **2010**. European buckthorn and Asian soybean aphid as components of an extensive invasional meltdown in North America. Biological Invasions. 12: 2913–2931.

Jenouvrier, S., H. Weimerskirch, C. Barbraud, Y.-H. Park, and B. Cazelles. **2005**. Evidence of a shift in the cyclicity of Antarctic seabird dynamics linked to climate. Proceedings of the Royal Society B: Biological Sciences. 272: 887–895.

Killick, R., and I. Eckley. **2014**. changepoint: An R package for changepoint analysis. Journal of Statistical Software. 58: 1–19.

Knapp, A. K., M. D. Smith, S. E. Hobbie, S. L. Collins, T. J. Fahey, G. J. A. Hansen, D. A. Landis, K. J. La Pierre, J. M. Melillo, T. R. Seastedt, G. R. Shaver, and J. R. Webster. **2012**. Past, present, and future roles of long-term experiments in the LTER Network. Bioscience. 62: 377–389.

Lovett, J. 2017. Monarch Population Status.

May, R. M. 1976. Simple mathematical models with very complicated dynamics. Nature. 261: 459–467.

Pleasants, J. M., and K. S. Oberhauser. **2013**. Milkweed loss in agricultural fields because of herbicide use: effect on the monarch butterfly population. Insect Conservation and Diversity. 6: 135–144.

Priyadarshana, W., and G. Sofronov. **2015**. Multiple break-points detection in array CGH data via the cross-entropy method. IEEE/ACM Transactions on Computational Biology and Bioinformatics (TCBB). 12: 487–498.

Prysby, M. D., and K. S. Oberhauser. **2004**. Temporal and geographic variation in monarch densities: citizen scientists document monarch population patterns. The monarch butterfly: Biology and conservation. 9–20.

R Development Core Team. **2017**. R: A Language and Environment for Statistical Computing 3.3.3. R Foundation for Statistical Computing.

Ragsdale, D. W., D. J. Voegtlin, and R. J. O'Neil. **2004**. Soybean aphid biology in North America. Annals of the Entomological Society of America. 97: 204–208.

Rhainds, M., H. J. S. Yoo, P. Kindlmann, D. Voegtlin, D. Castillo, C. Rutledge, C. Sadof, S. Yaninek, and R. J. O'Neil. **2010**. Two-year oscillation cycle in abundance of soybean aphid in Indiana. Agricultural and Forest Entomology. 12: 251–257.

Ricker, W. E. 1954. Stock and Recruitment. J. Fish. Res. Bd. Can. 11: 559–623.

Sarkar, S. 2017. What Is Threatening Monarchs? BioScience. 67: 1080–1080.

Saunders, S. P., L. Ries, K. S. Oberhauser, W. E. Thogmartin, and E. F. Zipkin. **2017**. Local and cross-seasonal associations of climate and land use with abundance of monarch butterflies Danaus plexippus. Ecography. n/a-n/a.

Sutherland, W. J., R. P. Freckleton, H. C. J. Godfray, S. R. Beissinger, T. Benton, D. D. Cameron, Y. Carmel, D. A. Coomes, T. Coulson, M. C. Emmerson, R. S. Hails, G. C. Hays, D. J. Hodgson, M. J. Hutchings, D. Johnson, J. P. G. Jones, M. J. Keeling, H. Kokko, W. E. Kunin, X. Lambin, O. T. Lewis, Y. Malhi, N. Mieszkowska, E. J. Milner-Gulland, K. Norris, A. B. Phillimore, D. W. Purves, J. M. Reid, D. C. Reuman, K. Thompson, J. M. J. Travis, L. A. Turnbull, D. A. Wardle, and T. Wiegand. **2013**. Identification of 100 fundamental ecological questions. J Ecol. 101: 58–67.

Toms, J. D., and M. L. Lesperance. **2003**. Piecewise regression: a tool for identifying ecological thresholds. Ecology. 84: 2034–2041.

Turchin, P. 2003. Complex population dynamics: a theoretical/empirical synthesis. Princeton University Press.

Urquhart, F. A., and N. R. Urquhart. **1978**. Autumnal migration routes of the eastern population of the monarch butterfly (Danaus p. plexippus L.; Danaidae; Lepidoptera) in North America to the overwintering site in the Neovolcanic Plateau of Mexico. Can. J. Zool. 56: 1759–1764.

Vidal, O., and E. Rendón-Salinas. **2014**. Dynamics and trends of overwintering colonies of the monarch butterfly in Mexico. Biological Conservation. 180: 165–175.

Weimerskirch, H., P. Inchausti, C. Guinet, and C. Barbraud. **2003**. Trends in bird and seal populations as indicators of a system shift in the Southern Ocean. Antarctic Science. 15: 249–256.

Wu, Z., D. Schenk-Hamlin, W. Zhan, D. W. Ragsdale, and G. E. Heimpel. **2004**. The soybean aphid in China: a historical review. Annals of the Entomological Society of America. 97: 209–218.

Zaya, D. N., I. S. Pearse, and G. Spyreas. **2017**. Long-Term Trends in Midwestern Milkweed Abundances and Their Relevance to Monarch Butterfly Declines. BioScience. 67: 343–356.

Zeileis, A., F. Leisch, K. Hornik, and C. Kleiber. **2001**. strucchange. An R package for testing for structural change in linear regression models.

Zipkin, E. F., C. E. Kraft, E. G. Cooch, and P. J. Sullivan. **2009**. When can efforts to control nuisance and invasive species backfire? Ecological Applications. 19: 1585–1595.

Zipkin, E. F., L. Ries, R. Reeves, J. Regetz, and K. S. Oberhauser. **2012**. Tracking climate impacts on the migratory monarch butterfly. Glob Change Biol. 18: 3039–3049.

Table 1: Ricker model parameter values for each phase between break points resulting from fitting population data of 1) multicolored Asian ladybeetles from Michigan, USA (1994-2017), and 2) the area occupied by monarch butterflies in their winter habitat in central Mexico (1995-2017). The parameter *r* is the per capita yearly intrinsic rate of increase and *K* is the carrying capacity (e.g., average number of adult ladybeetles captured per trap annually and hectares occupied by monarchs annually).

Species	**Years in subset**	***r* (± SE)**	***K* (± SE)**
Ladybeetle	1994-2000	1.3 ± 0.3	0.31 ± 0.02
Harmonia axyridis	2001-2005	2.3 ± 0.3	0.43 ± 0.03
	2006-2017	1.6 ± 0.3	0.27 ± 0.03
Monarch	1995-2003	1.0 ± 0.5	10.1 ± 1.9
Danaus plexippus	2004-2008	1.6 ± 0.2	5.6 ± 0.3
	2009-2017	1.2 ± 0.4	2.8 ± 0.5

Figure captions

Figure 1: Performance of the Regime Shift Detector (RSD) model under varying parameter values. Proportion of simulation results in which the true break scenario was detected within the top break point combinations as identified by the RSD implemented with an underlying Ricker model with varied A) noise (in the form of normally distributed error), B) starting values of the *r* parameter, C) percent changes in the *K* parameter, D) percent changes in *r*, and E) simulated time series length. Sets of 0, 1, 2 and 3 break points were randomly generated from within the set of possible values, and 250 datasets were simulated for each scenario. In each panel, other variables (that were not being varied) were held constant at their base values (i.e., noise=2%; starting value of $r = 2$; change in $r = \pm 25\%$; change in $K = \pm 75\%$; time series length = 20 years). Trends within a set of scenarios (grey lines) are illustrated with a third-order GAM smoothing line.

Figure 2: Average break weight of break points detected under varying parameterization conditions. Average weights of break points identified by the Regime Shift Detector model reflecting true parameterization conditions (diamonds) or erroneous breaks suggested by the model (triangles) under varied A) noise (in the form of normally distributed error), B) starting values of the *r* parameter, C) percent changes in the *K* parameter, D) percent changes in *r*, and E) simulated time series length. Sets of 0, 1, 2 and 3 break points were randomly generated from within the set of possible values, and 250 datasets were simulated for each scenario. In each panel, other variables (that were not being varied) were held constant at their base values (i.e., noise=2%; starting value of $r = 2$; change in $r = \pm 25\%$; change in $K = \pm 75\%$; time series length = 20 years). Trends within a set of scenarios (grey lines) are illustrated with a third-order GAM smoothing line.

Figure 3: Regime Shift Detector breaks and Ricker model fits for an invasive species. Population data documenting the invasion of multicolored Asian ladybeetle in Michigan, USA from 1994-2017. A) Time series data showing the average number of adults captured, per trap, per year. Vertical blue lines indicate years in which dynamic shifts occurred, as estimated by the Regime Shift Detector model. B) Ricker fits of time series data segments. Ladybeetle art by M. Broussard, used under a CC-BY 3.0 license.

Figure 4: Regime Shift Detector breaks and Ricker model fits for a species of conservation concern. Population data documenting the area occupied by monarch butterflies in their winter habitat in central Mexico from 1995-2017. A) Time series data showing the total area occupied by overwintering monarchs each year in December. Vertical blue lines indicate years in which dynamic shifts occurred, as estimated by the Regime Shift Detector model. B) Ricker fits of time series data segments. Butterfly art by D. Descouens and T.M. Seesey, used under a CC-BY 3.0 license.

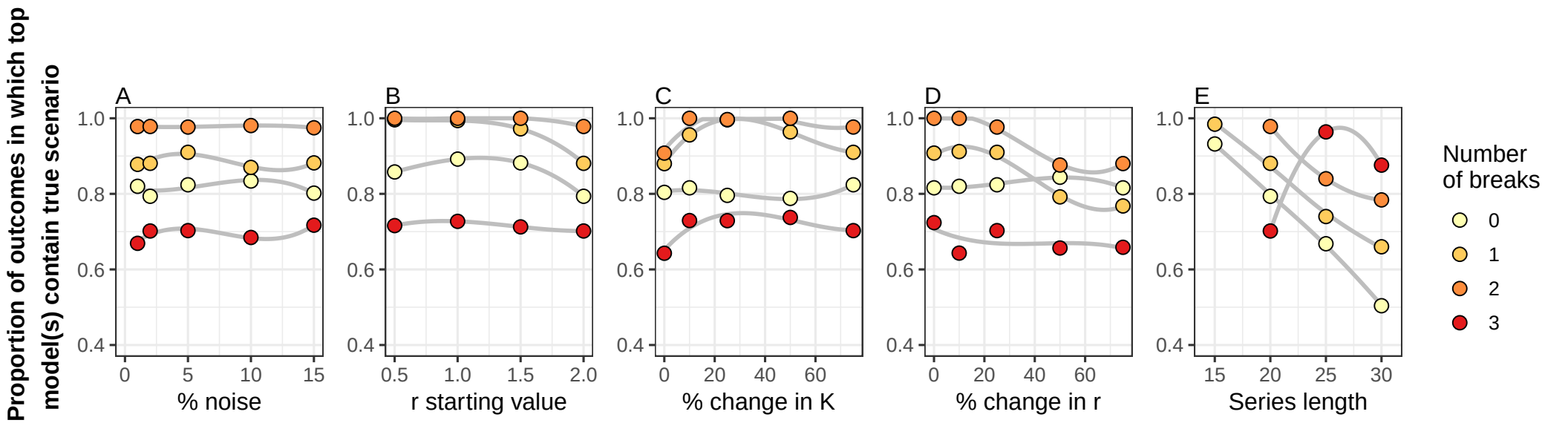
Proportion of outcomes in which top model(s) contain true scenario
A
B
C
D
E
1.0
0.8
0.6
0.4
0
5
10
15
% noise
0.5
1.0
1.5
2.0
r starting value
0
20
40
60
% change in K
% change in r
15
20
25
30
Series length
Number of breaks
0
1
2
3

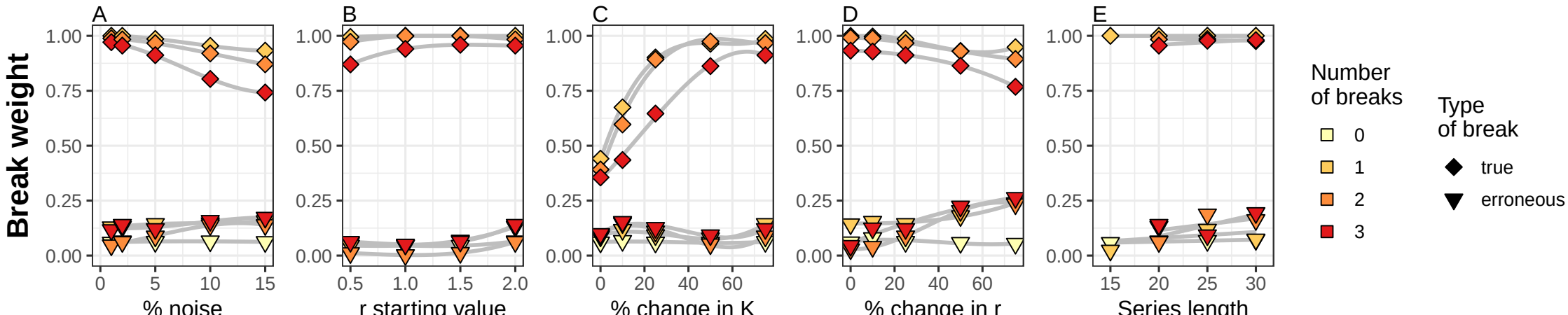
A
B
C
D
E
Break weight
1.00
0.75
0.50
0.25
0.00
0
5
10
15
% noise
0.5
1.0
1.5
2.0
r starting value
0
20
40
60
% change in K
% change in r
15
20
25
30
Series length
Number of breaks
0
1
2
3
Type of break
true
erroneous

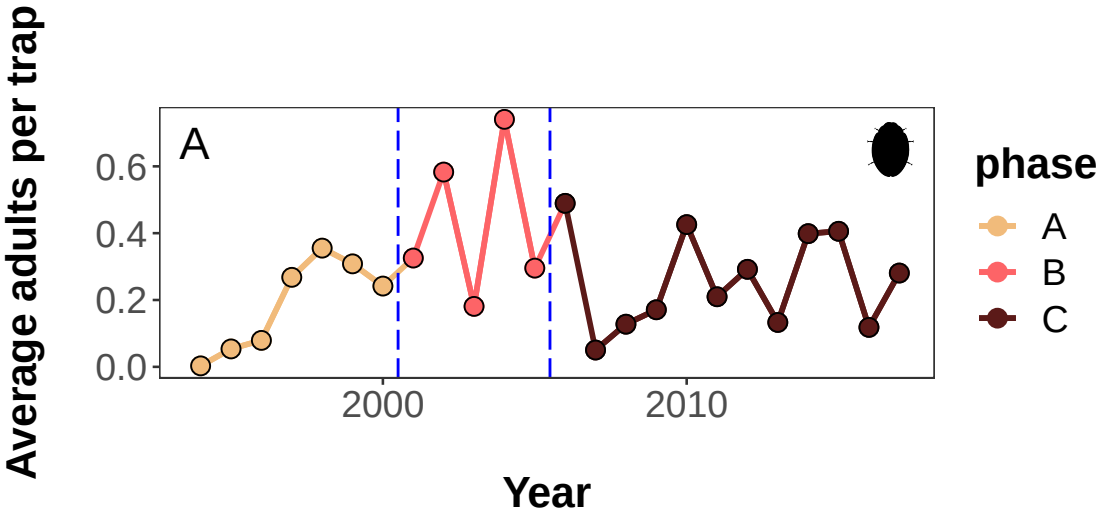
A
Average adults per trap
0.0
0.2
0.4
0.6
2000
2010
Year
phase
A
B
C

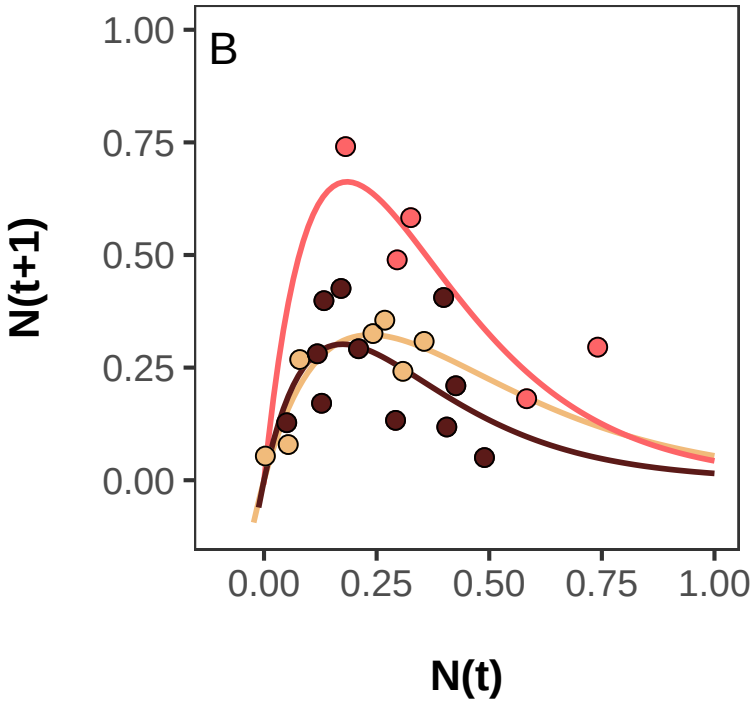
B
N(t+1)
0.00
0.25
0.50
0.75
1.00
N(t)

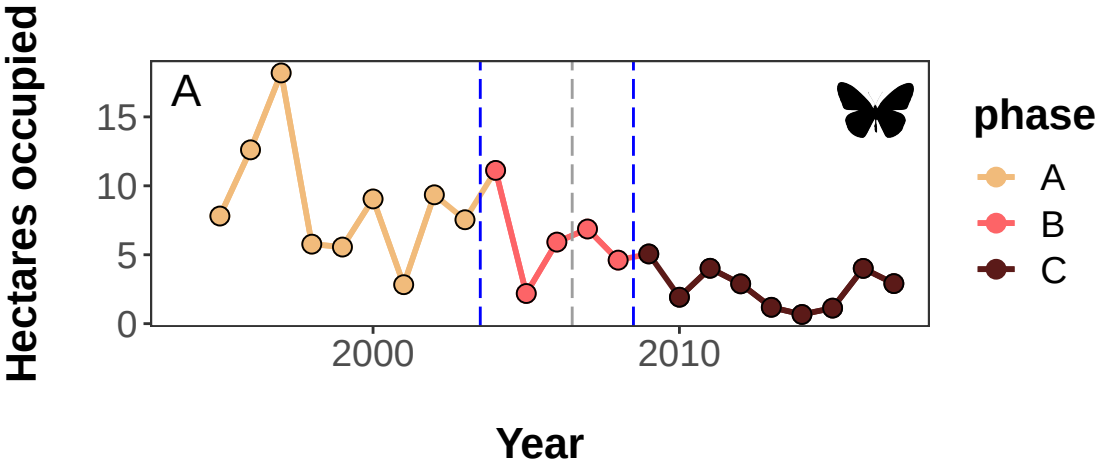
A
Hectares occupied
15
10
5
0
2000
2010
Year
phase
A
B
C

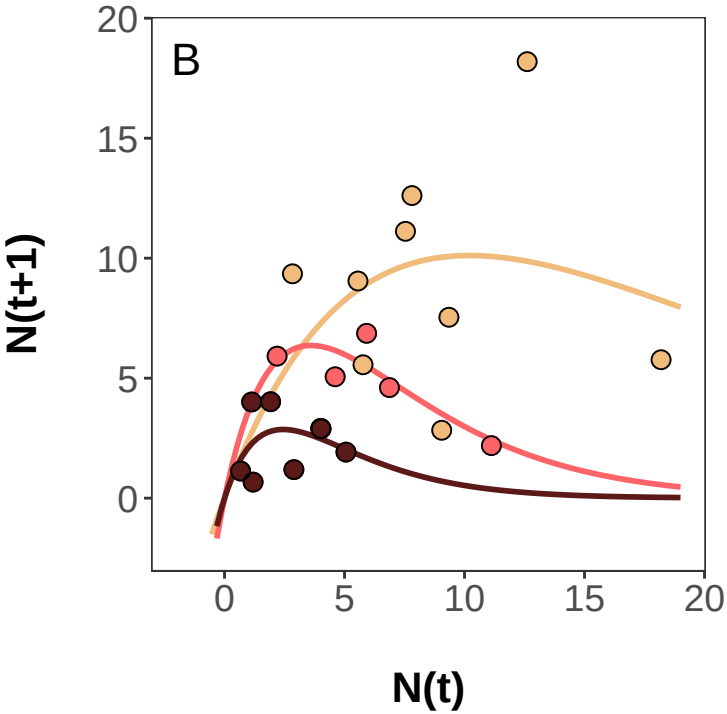
B
N(t+1)
20
15
10
5
0
0
5
10
15
20
N(t)